Kinetics of Capillary Condensation in Nanoscopic Sliding Friction

Elisa Riedo,[1] Francis Lévy,[2] and Harald Brune[1]

[1]*Institut de Physique des Nanostructures, Ecole Polytechnique Fédérale de Lausanne (EPFL), CH-1015 Lausanne, Switzerland*
[2]*Institut de Physique de la Matière Complexe, Ecole Polytechnique Fédérale de Lausanne (EPFL), CH-1015 Lausanne, Switzerland*
(Received 20 December 2001; published 18 April 2002)

The velocity and humidity dependence of nanoscopic sliding friction has been studied on CrN and diamondlike carbon surfaces with an atomic force microscope. The surface wettability is found to be decisive. Partially hydrophilic surfaces show a logarithmic decrease of friction with increasing velocity, the slope of which varies drastically with humidity, whereas on partially hydrophobic surfaces we confirm the formerly reported logarithmic increase. A model for the thermally activated nucleation of water bridges between tip and sample asperities fully reproduces the experimental data.

DOI: 10.1103/PhysRevLett.88.185505 PACS numbers: 81.40.Pq, 07.79.Lh, 46.55.+d, 68.35.Np

Sliding friction is an everyday life issue, and its universal nature emerges from the great variety of industrial processes and natural phenomena in which it plays a central role [1,2]. The fundamental understanding of sliding friction and adhesion forces is crucial in fields as widespread as earthquake dynamics [1] and preplanetary dust aggregation [3]. With the miniaturization of moving components in many technological devices, such as microelectromechanical systems and hard disks, it has become of primary importance to study surface forces such as friction, viscous drag, and adhesion at microscales and nanoscales. Compared to its scientific and technological importance, only little is known about the mechanisms giving rise to the observed velocity dependence of nanoscopic friction [1,4–12]; in particular, the role played by humidity in this dependence has not yet been highlighted.

Current literature results on the velocity dependence of nanoscopic friction are highly controversial. Experiments performed under ambient conditions reported a manifold of material dependent behaviors, going from a logarithmic increase of friction force with increasing velocity all the way down to a steep logarithmic decrease [12]; also no variation at all has been reported [13]. Experiments carried out under ultrahigh vacuum (UHV) [5], as well as under controlled atmosphere [6], showed a logarithmic increase of nanoscopic friction. The origin of these different velocity dependencies is far from being understood. The logarithmic increase under UHV and controlled atmosphere has recently been attributed to a temperature dependent stick and slip motion [5,6]. While this attribution may require further substantiation, it is certainly better understood than the wealth of behaviors observed under ambient conditions. It has been suggested that under ambient conditions capillary forces could play a role [12]; however, the experimental proof of this idea and a quantitative model of capillary condensation explaining all observed velocity dependencies of sliding friction were thus far lacking.

In this Letter, we demonstrate that the forces in sliding friction are determined by the superposition of two competitive phenomena, both having logarithmic velocity dependence, but with opposite slopes. The first is stick and slip motion giving rise to a logarithmic increase of friction with increasing velocity. The second is due to the kinetics of capillary condensation of water vapor in the contact area between the two sliding bodies and causes a logarithmic decrease of friction with increasing velocity. Consequently, the degree of wettability and the ambient humidity determine whether one or the other dominates and whether the overall slope is positive or negative. In line with this idea, we observe that the slope can be varied substantially by changing the relative humidity. We present a model which perfectly reproduces the measured humidity and velocity dependence of the sliding friction on partially hydrophilic and hydrophobic surfaces. Furthermore, this model enables access to the microscopic quantities involved in capillary condensation via measurement of the sliding friction force.

For our study, we selected samples customarily used in hard coating technology where small friction forces are required. The samples were CrN [14] and diamondlike carbon (DLC) films [15]. The CrN films have been deposited at 24 °C (LT-CrN) and 500 °C (HT-CrN) substrate temperature [14]. The different growth temperatures lead to a different wettability as evidenced by static water contact angles of $\theta_c = 93°$ (LT-CrN) and $\theta_c = 45°$ (HT-CrN) [16]. These values are commonly associated with more hydrophobic and less hydrophobic surfaces, respectively. For contrast, we chose the expressions partially hydrophobic and partially hydrophilic throughout this Letter. DLC is partially hydrophobic with $\theta_c = 85°$. While the DLC films are extremely smooth, the CrN films are rough for both growth temperatures (the root mean square roughnesses on 1 μm^2 for DLC, LT-CrN, and HT-CrN are 0.2, 5.5, and 3.7 nm, respectively) [15].

The friction forces and the surface topography of the films were investigated at room temperature by means of an atomic force microscope (AFM) (AutoProbe^{TM} M5). For humidity control, the AFM was placed in a tight box with inlets for dry and water saturated nitrogen. We used V-shaped silicon cantilevers, and silicon conical tips [17]. The normal and friction forces, F_N and F_F, are proportional to the normal and the lateral deflections of the

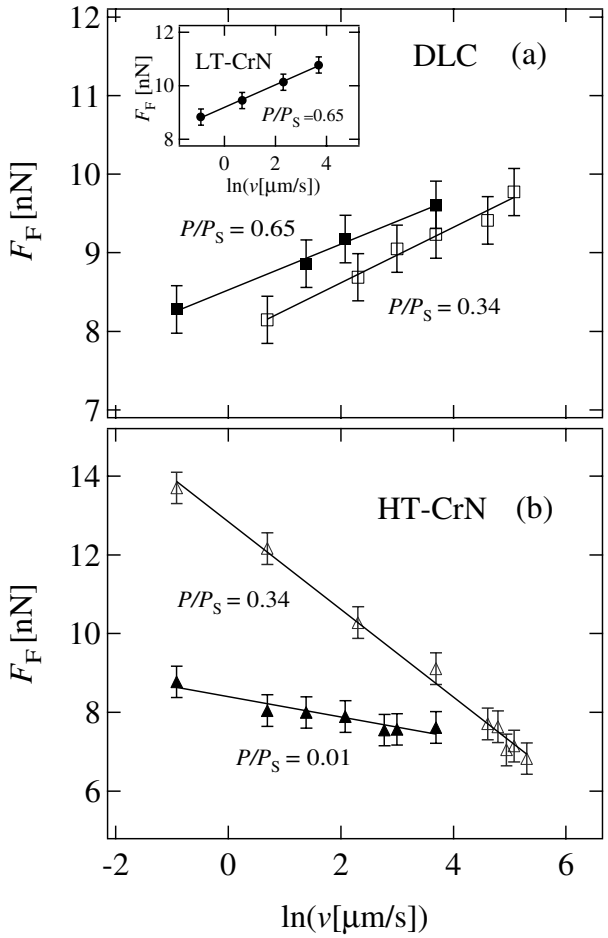

FIG. 1. (a) F_F as a function of sliding velocity for partially hydrophobic surfaces. Main figure: DLC at relative humidities $P/P_S = 0.34$ and 0.65 (P is the vapor pressure and P_S the saturated vapor pressure). Inset: LT-CrN films at $P/P_S = 0.65$. (b) $F_F(v)$ for a partially hydrophilic surface (HT-CrN) at $P/P_S = 0.01$ and 0.34. In (a) and (b), $F_N = 12.2$ nN.

cantilever which are recorded simultaneously. We define $F_N = 0$ nN at the point where the cantilever is not bent. Force calibration was achieved by calculating the normal and torsional spring constants, k_n and k_t, from the cantilever geometry, the thickness being inferred from the resonance frequency [18,19]. The spring constants obtained in this way are $k_n = 0.35 \pm 0.05$ N/m and $k_t = 75 \pm 10$ N/m. Our knowledge on k_n and k_t determines the absolute accuracy of the measured forces; however, their relative changes were determined more accurately by using the same cantilever throughout a series of experiments. The velocity dependence of friction was investigated in varying the scan frequency at fixed size. We verified that varying the scan size at constant frequency yielded consistent results.

The velocity, v, dependence of friction force F_F is shown in Fig. 1. For all samples and humidities, there is a linear variation of F_F with $\ln(v)$, expressed as follows:

$$F_F = F_{0v} + F_{1v} \ln(v[\mu m/s]), \quad (1)$$

TABLE I. Results from the line fits shown in Fig. 1.

	DLC		LT-CrN	HT-CrN	
P/P_S	0.34	0.65	0.34	0.01	0.34
F_{1v} [nN]	0.35(2)	0.23(2)	0.42(1)	−0.29(4)	−1.00(5)
F_{0v} [nN]	7.9(1)	8.54(4)	9.20(3)	8.4(1)	12.6(2)

where F_{1v} is the slope and F_{0v} the intercept of the line fits shown in Fig. 1. The logarithmic variation of F_F with v is in agreement with literature [5,6,12]. However, our results show that the sign of the slope is determined by the wettability of the surface. Partially hydrophobic surfaces are characterized by positive slopes, whereas $dF_F/d\ln v$ is negative on partially hydrophilic surfaces. The importance of surface wettability and relative humidity in sliding friction is evidenced particularly clearly, and for the first time, by the observation that the slope on the very same sample can be varied by changing humidity. As expected, this variation is larger (up to a factor of 3, see Fig. 1b) for a partially hydrophilic sample than for a partially hydrophobic one (Fig. 1a). In both cases, the effect of a humidity increase is to add a negative value to the slope (see Table I).

First insight in the origin of the slope variation can be gained from Fig. 2, showing the humidity dependence of sliding friction for HT-CrN films. Friction forces increase with relative humidity in the way expressed by the following empirical law:

$$F_F = F_{0p} + F_{1p} \frac{1}{\ln \frac{P_S}{P}}. \quad (2)$$

The data reported for native oxide covered Si(100) in Ref. [12] equally obey Eq. (2), as seen in the lower inset [20]. Both surfaces are partially hydrophilic. Our HT-CrN

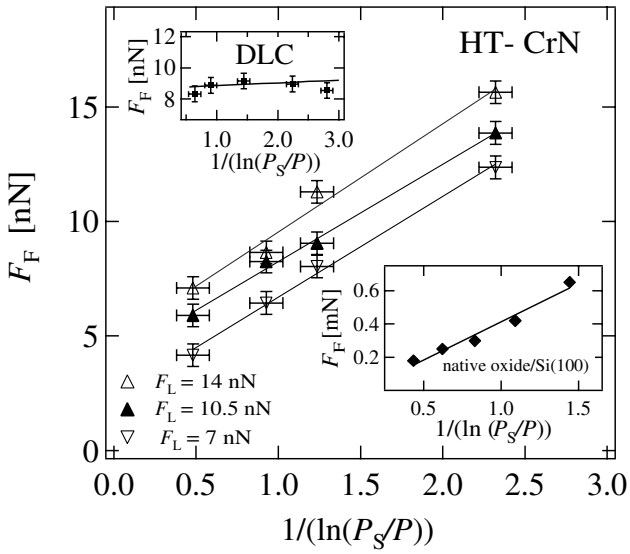

FIG. 2. F_F as a function of P/P_S at $v = 10$ μm/s and different normal loads for HT-CrN films. The solid lines represent linear fits to the experimental data with Eq. (2). The insets show $F_F(P/P_S)$ for DLC and native oxide covered Si films.

TABLE II. Results from the linear fits in Fig. 2 for HT-CrN.

F_N [nN]	F_{1p} [nN]	F_{0p} [nN]
14.0	4.7(4)	4.8(6)
10.5	4.3(2)	4.0(3)
7.0	4.4(2)	2.3(3)

data reveal further that the slope F_{1p} is almost unaffected by the normal load F_N, whereas the overall friction force, i.e., the offset F_{0p}, increases with load (see Table II). On the partially hydrophobic DLC surface, F_F is largely independent of humidity (see upper inset).

The observed variation of the friction force with humidity can have two origins. It can be due to a variation of the adhesion force or to a variation of the friction coefficient, μ. The relationship between friction and normal forces is for a multiasperity contact [1,21]:

$$F_F = \mu(F_N + F_{adh}). \quad (3)$$

Our F_F versus F_N measurements on HT-CrN films confirm the linear behavior expressed in Eq. (3) at various humidities. As shown in Table III, μ at fixed velocity remains largely unaffected by changing humidity; hence, the variation of friction forces with humidity can almost entirely be attributed to the variation of adhesion forces.

In order to explain the observed behavior, we developed a model which fully reproduces Eqs. (1) and (2) and establishes a relationship of the appearing quantities F_{0v}, F_{1v}, F_{0p}, and F_{1p} with the microscopic parameters involved. We first consider two perfectly smooth surfaces, namely, a spherically shaped tip and a flat sample in mutual mechanical contact. In the presence of humidity, F_{adh} is the sum of the capillary force F_c, due to the Laplace pressure of the water meniscus forming between the tip and the sample, and the direct adhesion F_{ss} of the two contacting solids within the liquid [8,22]:

$$F_{adh} = F_{ss} + F_c. \quad (4)$$

For a spherically shaped meniscus, F_c can be written as

$$F_c \approx 2\pi R_t \gamma(\cos\theta_s + \cos\theta_t), \quad (5)$$

where R_t is the tip radius, γ is the surface tension of water, and θ_s and θ_t are the static contact angles of the sample and the tip, respectively. From inspection of Eq. (5), it is clear that F_c and with it F_{adh} have no humidity dependence. Hence, on perfectly smooth surfaces, one expects two discrete humidity regimes, each with constant friction force. For small humidities, there is no meniscus and $F_{adh} = F_{ss}$, and from a certain threshold humidity on a single meniscus forms giving rise to a larger but constant adhesion force. If one considers surface roughness, however, there may arise a pronounced and continuous humidity dependence.

TABLE III. Results from the fits to our data with Eq. (3).

P/P_S	μ	F_{adh} [nN]
0.12	0.44(3)	2.7(7)
0.44	0.45(1)	15.5(2)
0.68	0.40(2)	23.5(5)

Our starting point is a model developed by Bocquet *et al.* in order to explain the observed increase of macroscopic static friction with the time during which two solids remain in contact [23]. Everybody has experienced that the stability of sand castles increases when the wet sand is pressed into shape for a longer time. In the cited model, the number of capillary bridges forming between the solids increases with the contact time, giving rise to an increase in adhesion force and in the strength of static friction. We propose that a similar effect can be observed in the dynamic case of sliding friction and at a nanoscopic scale. We consider first the length scale for capillary condensation. The Kelvin radius, R_K, is the radius of curvature of a water meniscus at equilibrium [22] (see Fig. 3). Under ambient conditions R_K is about 1 nm [22], and, as a consequence, liquid bridges are able to condense only in nanometer-scale interstices. In the situation represented in Fig. 3, one gap of height h defines the volume of a potential liquid bridge $V = hA$, where A is the bridge cross section which we consider as a constant for simplicity. The condensation of such a liquid bridge costs a threshold free energy $\Delta E(h) = k_B T \ln(P_S/P) hA\rho$, where ρ is the molecular density of the liquid in units molecules/m^3. Assuming an activation process, the time needed to form a bridge of height h is $t(h) = t_A \exp[\Delta E(h)/k_B T]$, where t_A is the condensation time of a liquid monolayer. From $t(h)$, we can find the maximum height where a liquid bridge can form after a time t, $h_{max}(t) = \ln(t/t_A)[\ln(P_S/P)A\rho]^{-1}$. Because of roughness, nucleating sites exhibit a broad height distribution and only a fraction $f(t)$ of the total number of liquid bridges is indeed formed at a given time. To a first approximation, the fraction of nucleating sites with $h < h_{max}$ is equal to $f(t) = h_{max}(t)/\lambda$, with λ being the full width of the interstitial height distribution [23].

With surface roughness taken into account, the capillary force becomes a continuous function of the time the sliding surfaces spend in contact, and F_c in Eqs. (4) and (5) gets multiplied by $f(t)$. Upon sliding of two surfaces on top of each other with velocity v, the residence time of a contact with diameter d is $t = d/v$. As sliding velocity is

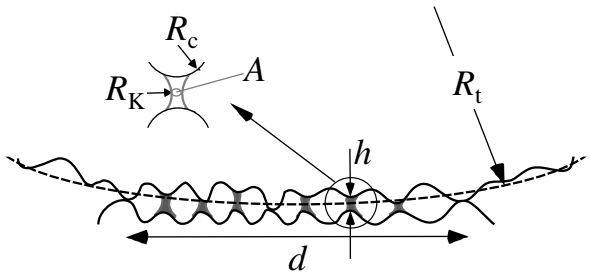

FIG. 3. Capillary water bridges with height h, forming in the contact area, with diameter d, between the AFM tip and the sample. The tip, capillary, and Kelvin radii are R_t, R_c, R_K, respectively; the cross section of the capillary bridges is A.

decreased, there is a continuous increase of the number of capillary bridges forming in the area of contact.

We discussed above that the overall friction force is given by superposition of the stick and slip related increase and the capillary condensation related decrease of friction with velocity. The first gives rise to a term $m\ln(v/v_B)$, with $m > 0$ and v_B being a characteristic velocity [5,6], and the second contribution is obtained from combining Eqs. (5) [multiplied by $f(t)$] (4), and (3). This yields the following for the total friction force:

$$\begin{aligned} F_F &= \mu(F_N + F_{ss}) + \mu[F_c f(t)] + m\ln\left(\frac{v}{v_B}\right) \\ &= \mu(F_N + F_{ss}) - \mu[2\pi R_t \gamma(\cos\theta_s + \cos\theta_t)] \\ &\quad \times \left(\frac{1}{\lambda A\rho}\,\frac{1}{\ln\frac{P_S}{P}}\right)\ln\frac{v}{v_A} + m\ln\left(\frac{v}{v_B}\right), \end{aligned} \tag{6}$$

where v_A is defined as d/t_A. One recognizes the $\ln(v)$ dependence at constant P/P_S and the $1/\ln(P_S/P)$ dependence at constant v; thus Eqs. (1) and (2) are reproduced. Furthermore, the model establishes a relationship between measured slopes and intercepts and microscopic quantities as the cross section and the condensation time of a capillary bridge, or as the static contact angle of the AFM tip. By combining the measured static contact angles of the various samples with the results shown in Tables I and II, we can determine the values of the following parameters: $F_c/\lambda A\rho$, v_A, and m (see Table IV).

It is seen that the slope due to stick and slip motion is roughly identical for all samples. The characteristic velocity for capillary condensation v_A is identical on all samples and leads with $d \approx 10$ nm (as estimated from R_t, see below) to an experimental estimate of the condensation time for one liquid layer $t_A = d/v_A = 25\ \mu$s. It has been anticipated that this time should be of the order of microseconds [23], but, to our knowledge thus far, there existed no experimental estimate of this number. The hydrophobicity of the AFM tip can be estimated from the ratio between $F_c/\lambda A\rho$ on DLC and on HT-CrN. This ratio equals $(\cos\theta_{DLC} + \cos\theta_t)/(\cos\theta_{HT\text{-}CrN} + \cos\theta_t)$ leading to $\theta_t = 90°$. This is higher than expected for a native oxide covered Si tip and is close to the one of clean Si. This finding is consistent with Ref. [8] and may be indicative of partial oxide removal during sliding. Since there is only a finite number of capillary bridges that can be formed for a given contact diameter and roughness, the friction force must saturate upon increase of humidity for a given velocity or upon decrease of velocity for a given humidity. We confirm this saturation, e.g., for HT-CrN, where we find that F_F saturates at $P/P_S \geq 0.75$ for $v = 10\ \mu$m/s; we equally expect saturation for $v \leq 1$ nm at $P/P_S = 0.34$. The observed saturation value can be used to estimate the cross section of a liquid bridge A; assuming that $\lambda \approx 1$ nm, we get $A \approx 0.4$ nm^2. Finally, we can estimate the radius of curvature of the AFM tip from knowledge of A, $F_c/\lambda A\rho$, and v_A. We consistently find $R_t \approx 100$ nm for each of the surfaces.

TABLE IV. Comparison of Eq. (6) with Tables I and II.

	DLC	LT-CrN	HT-CrN
$F_c/\lambda A\rho$ [nN]	0.3(1)	0.2(1)	3.0(2)
m	0.39	0.33	0.30
v_A [μm/s]	400(50)	400(50)	400(50)

In conclusion, we showed that for partially hydrophilic and nanometer-scale rough surfaces friction decreases logarithmically with the scan velocity, whereas for partially hydrophobic surfaces nanoscale friction increases with velocity. The experimentally found logarithmic variations of friction force with sliding velocity and relative humidity have been fully explained with a model based on the kinetics of capillary condensation.

We acknowledge A. Kulik for experimental support.

[1] B. N. J. Persson, *Sliding Friction: Physical Principles and Applications* (Springer-Verlag, Berlin, 2000).
[2] E. Meyer *et al., Nanoscience: Friction and Rheology on the Nanometer Scale* (World Scientific, Singapore, 1998).
[3] L. O. Heim *et al.,* Phys. Rev. Lett. **83**, 3328 (1999).
[4] J. F. Joanny and M. O. Robbins, J. Chem. Phys. **92**, 3206 (1990).
[5] E. Gnecco *et al.,* Phys. Rev. Lett. **84**, 1172 (2000).
[6] T. Bouhacina *et al.,* Phys. Rev. B **56**, 7694 (1997).
[7] T. Stifter, O. Marti, and B. Bhushan, Phys. Rev. B **62**, 13 667 (2000).
[8] Y. Ando, Wear **238**, 12 (2000).
[9] B. Bhushan and C. Dandavate, J. Appl. Phys. **87**, 1201 (2000).
[10] M. Binggeli and C. M. Mate, Appl. Phys. Lett. **65**, 415 (1994).
[11] R. Prioli, D. C. Reigada, and F. L. Freire, J. Appl. Phys. **88**, 679 (2000).
[12] H. Liu, S. I.-U. Ahmed, and M. Scherge, Thin Solid Films **381**, 135 (2001).
[13] O. Zwörner *et al.,* Appl. Phys. A **66**, S263 (1998).
[14] P. Hones, R. Sanjinés, and F. Lévy, Surf. Coat. Technol. **95/5**, 398 (1997).
[15] E. Riedo *et al.,* Surf. Sci. **477**, 25 (2001).
[16] Advancing and receding contact angles for HT-CrN and LT-CrN are, respectively, $\theta_a = 52°, 94°$ and $\theta_r = 25°, 45°$.
[17] We used triangular cantilevers (Ultralevers B). Their dimensions were derived using an optical microscope.
[18] R. Lüthi *et al.,* Surf. Sci. **338**, 247 (1995).
[19] J. M. Neumeister and W. A. Ducker, Rev. Sci. Instrum. **65**, 2527 (1994).
[20] This sample showed a linear decrease of F_F with $\ln v$.
[21] C. A. J. Putman, M. Igarashi, and R. Kaneko, Appl. Phys. Lett. **66**, 3221 (1995).
[22] J. Israelachvili, *Intermolecular and Surface Forces* (Academic Press, San Diego, 1997).
[23] L. Bocquet *et al.,* Nature (London) **396**, 735 (1998).